Available online at www.sciencedirect.com
SCIENCE DIRECT®
Bioorganic & Medicinal Chemistry 12 (2004) 3229–3237
Bioorganic & Medicinal Chemistry

Radiosynthesis and pharmacological evaluation of [^{11}C]EMD-95885: a high affinity ligand for NR2B-containing NMDA receptors

G. Roger,[a] F. Dollé,[a] B. de Bruin,[a] X. Liu,[b] L. Besret,[c] Y. Bramoullé,[a] C. Coulon,[a] M. Ottaviani,[a] M. Bottlaender,[a] H. Valette[a] and M. Kassiou[b,d,*]

[a]*Service Hospitalier Frédéric Joliot, Département de Recherche Médicale, CEA/DSV, 4 Place du Général Leclerc, F-91401 Orsay, France*
[b]*Department of Pharmacology, University of Sydney, Sydney NSW 2006, Australia*
[c]*URA CEA/CNRS 2210, Service Hospitalier Frédéric Joliot, Département de Recherche Médicale, CEA/DSV, 4 Place du Général Leclerc, F-91401 Orsay, France*
[d]*Department of PET and Nuclear Medicine, Royal Prince Alfred Hospital, Missenden Road, Camperdown, Sydney NSW 2050, Australia*

Received 5 February 2004; revised 29 March 2004; accepted 30 March 2004
Available online 10 May 2004

Abstract—EMD-95885, 6-[3-[4-(4-fluorobenzyl)piperidino]propionyl]-3*H*-benzoxazol-2-one (**1**) has been described as a selective antagonist for the NMDA receptors containing NR2B subunits, displaying an IC_{50} of 3.9 nM for this subtype. EMD-95885 (**1**) has been synthesized in good overall yield and labelled with carbon-11 ($T_{1/2}$: 20.4 min) at its benzoxazolinone moiety using [^{11}C]phosgene. The pharmacological profile of [^{11}C]EMD-95885 ([^{11}C]-**1**) was evaluated in vivo in rats with biodistribution studies and brain radioactivity monitored with intracerebral radiosensitive β-microprobes. The brain uptake of [^{11}C]-**1** was homogeneous (0.4–0.6% ID/mL) across the different brain structures studied. This in vivo brain regional distribution of [^{11}C]-**1** was not consistent with the known distribution of NR2B subunits. Also as a measure of specificity the hippocampus/cerebellum ratio reached 0.8 throughout the time course of the experiment supporting the lack of specificity. Competition studies with the NR2B prototypic ligand ifenprodil and EMD-95885 (**1**), 30 min before the radioligand injection, displayed homogeneous reduction of [^{11}C]-**1** uptake of 40–60%. Pre-treatment of rats with DTG (σ ligand), MDL105519 (glycine site antagonist) and MK801 (ion channel blocker) had no inhibitory effect on [^{11}C]-**1** uptake. Use of haloperidol as a blocking drug also resulted in a homogeneous inhibition of [^{11}C]-**1** uptake by 66–60%, which does not reflect binding to dopamine or σ receptors. Due to the homogeneous radioligand uptake and inhibition and no measure of cerebral blood flow effects during these blocking studies it is uncertain whether any specific binding is observed. In view of these results, [^{11}C]EMD-95885 ([^{11}C]-**1**) does not have the required properties for imaging NR2B containing NMDA receptors using positron emission tomography.

1. Introduction

The *N*-methyl-D-aspartate (NMDA) receptor is a ligand gated ion channel with the channel opening triggered by synaptically released glutamate, the principal excitatory neurotransmitter in the CNS.[1] However, binding of glycine, a co-agonist, is required for receptor activation.[2] Allosteric modulators, which include protons, polyamines, Zn^{2+}, Mg^{2+} and redox reagents also affect receptor activity.[1] Functional NMDA receptors are heteromers composed of both members of the two subunit families, namely NR1 (eight different splice variants) and NR2 (A–D) subunits.[3] The NR2 subunits contain glutamate binding sites[4] whereas the NR1 subunits contain the glycine binding site.[5] The subunit composition of the NMDA receptor confers diverse functional properties along with significant effect on the sensitivity of the allosteric modulators.

NMDA receptors mediate a number of physiological and pathophysiological processes in the mammalian CNS. Abnormal expression, function or regulation of NMDA receptors is involved in a number of neurodegenerative and psychiatric disorders.[1,6] Therefore, ligands that block or reduce the activity of NMDA receptors should be useful as neuroprotective agents,

Keywords: EMD-95885; NMDA receptor; NR2B subunit; Carbon-11; Positron emission tomography (PET).
* Corresponding author. Tel.: +61-2-9515-5150; fax: +61-2-9515-6381; e-mail: mkassiou@med.usyd.edu.au

0968-0896/$ - see front matter © 2004 Elsevier Ltd. All rights reserved.
doi:10.1016/j.bmc.2004.03.065

anticonvulsants, analgesics and possibly for the therapy of motor disorders such as Parkinson's disease.[7] The hypothesis that excessive activation of NMDA receptors is involved with a number of neurodegenerative and psychiatric disorders has generated extensive interest in the NMDA receptor as a target for new pharmacotherapies. However, the contribution of NMDA receptor subtypes in these disorders is not well understood due to the lack of subunit selective drugs. This deficiency is currently been addressed since the discovery of the prototypic NR2B subunit selective antagonist ifenprodil.[8,9]

Introduction of noninvasive imaging techniques such as positron emission tomography (PET) has made possible the study of neuroreceptors in the living human brain. Such studies have proven useful in the localization and quantification of neuroreceptors and offer insight into the relationship of these receptors in normal and pathological states.[10] Attempts to image NMDA receptors using PET have mainly focused on development of carbon-11-labelled radioligands for the glycine binding site[11–14] and the ion channel,[15–19] which have proved unsuccessful. Recently, ifenprodil analogues selective for the NR2B subunit have also been radiolabelled and evaluated which include (±)*threo*-1-(4-hydroxyphenyl)-2[4-hydroxy-4-(*p*-[^{11}C]methoxyphenyl)piperidino]-1-propanol ([^{11}C]CP-101,606) ($IC_{50} = 10$ nM for protection against glutamate toxicity)[20] and 5-[3-(4-benzylpiperidin-1-yl)prop-1-ynyl]-1,3-dihydrobenzoimidazol-2-[^{11}C]one ($IC_{50} = 5.3$ nM for inhibition of NMDA responses).[21] Even though both radioligands display in vitro selectivity for the NR2B subunit, this selectivity was not observed in vivo.

Further optimization of ifenprodil for better selectivity and potency has resulted in the discovery of 6-[3-[4-(4-fluorobenzyl)piperidino]propionyl]-3*H*-benzoxazol-2-one (EMD-95885, **1**).[22] This compound was reported to have high affinity for the NR2B subunit ($IC_{50} = 3.9$ nM) and does not interact with other sites on the NMDA receptor. Its benzoxazolinone structure permits its radiolabelling with carbon-11 in the form of [^{11}C]phosgene and therefore was considered an appropriate candidate for potential imaging of NMDA receptors containing NR2B subunits.

The present work represents (a) a concise synthesis of EMD-95885 (**1**), as the nonradioactive reference and its precursor **2** for radiolabelling; (b) the labelling of **1** with [^{11}C]phosgene at the benzoxazolinone moiety; (c) the in vivo evaluation of this radioligand in rodents in biodistribution studies and brain radioactivity monitoring with intracerebral radiosensitive β-microprobes.

2. Results and discussion

2.1. Chemistry

6-[3-[4-(4-Fluorobenzyl)piperidino]propionyl]-3*H*-benzoxazol-2-one (EMD-95885, **1**, as reference) and 1-(4-fluorobenzyl)piperidin-1-yl]propan-1-one (**2**, radiolabelling precursor) were synthesized in two and four chemical steps, respectively (Schemes 1 and 2). Both compounds were synthesized according to literature procedures.[23–25]

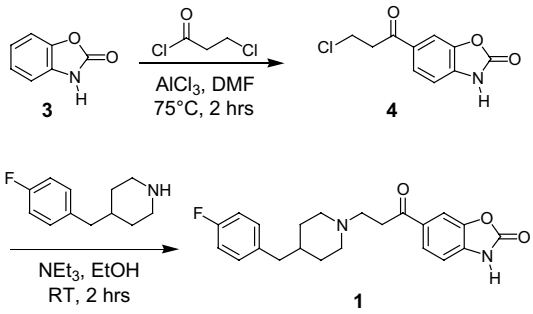

Scheme 1. Synthesis of 6-[3-[4-(4-fluorobenzyl)piperidino]propionyl]-3*H*-benzoxazol-2-one (EMD-95885) (**1**).

Commercially available 2-benzoxazolinone **3**, was added to a mixture of aluminium chloride and DMF followed by 3-chloropropionyl chloride resulting in the formation of 6-(3-chloropropionyl)-3*H*-benzoxazol-2-one **4** in 29% yield.[25] Compound **4** was then treated with 4-(4-fluorobenzyl)piperidine in ethanol containing triethylamine to yield the title compound **1** in 65% yield.[23]

The hydrolysis of the benzoxazolinone moiety of **1** in alkaline conditions,[26,27] 10% KOH in ethanol stirring at room temperature for 3 h, failed to yield the radiolabelling precursor **2**. A complex mixture of products resulted in which **2** could not be identified or isolated. A two step approach was found to be more successful with the initial step involving formation of the carbamate **5** from the reaction of **1** with di-*tert*-butyl dicarbonate in THF in the presence of nucleophilic addition catalyst dimethylaminopyridine (DMAP) at room temperature for 1.5 h.[24] The *t*-Boc group was removed by treating **5** with trifluoroacetic acid resulting in the radiolabelling precursor **2** in 80% yield.

2.2. Radiochemistry

The benzoxazolinone **1** was labelled with carbon-11 ($T_{1/2}$: 20.4 min) using no-carrier-added [^{11}C]phosgene and the aminohydroxyphenyl precursor **2** (Schemes 3 and 4).

[^{11}C]Phosgene ([^{11}C]$COCl_2$) was synthesized from cyclotron-produced [^{11}C]methane ([^{11}C]CH_4) via [^{11}C]carbon tetrachloride ([^{11}C]CCl_4) using minor modifications of published processes (Scheme 3).[28–31] Briefly, [^{11}C]CH_4 was separated from the target contents, trapped and concentrated on Porapak-Q. [^{11}C]CH_4 was then carried off by a flow of helium gas, mixed with 3 mL of chlorine and the mixture passed through an empty linear horizontal glass tube at a temperature of 510 °C.[30] The on-line synthesized [^{11}C]CCl_4 was continuously swept away by the same helium vector gas and finally passed through a glass-U-tube containing iron filings at a temperature of 290–310 °C,[31] without intentional addi-

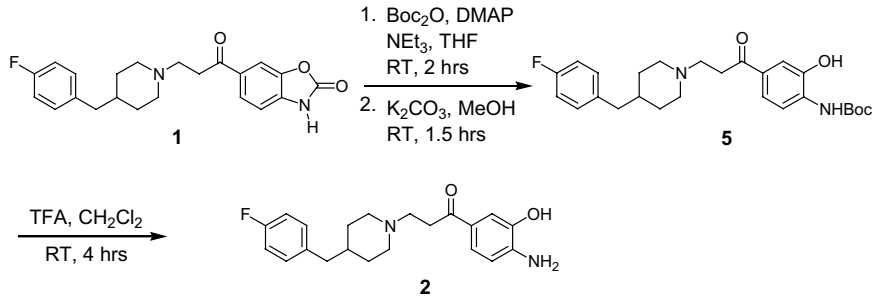

Scheme 2. Synthesis of the radiolabelling precursor 1-(4-amino-3-hydroxy-phenyl)-3-[4-(4-fluorobenzyl)piperidin-1-yl]propan-1-one (**2**).

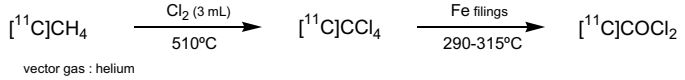

Scheme 3. Preparation of [^{11}C]phosgene from [^{11}C]methane.

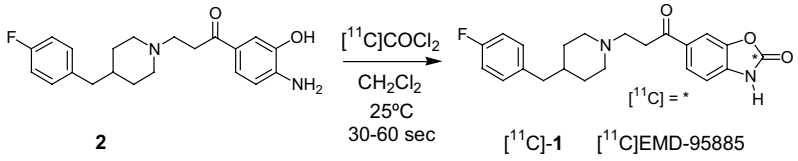

Scheme 4. Radiosynthesis of 6-[3-[4-(4-fluorobenzyl)piperidino]propionyl]-3*H*-benzoxazol-2-[^{11}C]one ([^{11}C]EMD-95885, [^{11}C]-**1**).

tion of oxygen to the system, giving [^{11}C]$COCl_2$ in 12–13 min and an average of 30–50% decay-corrected radiochemical yield, based on starting [^{11}C]CH_4.

[^{11}C]$COCl_2$ was trapped (bubbling through) at room temperature in CH_2Cl_2 (500 μL) containing the labelling precursor **2** (0.5–1.0 mg) (Scheme 4). The cyclization reaction of [^{11}C]phosgene was fast (almost instantaneously), but gave [^{11}C]-**1** in low radiochemical yields. Typically, starting from a 1.2 Ci (44.4 GBq) [^{11}C]CH_4 production batch, 10–20 mCi (0.37–0.74 GBq) of [^{11}C]-**1** with a radiochemical- and chemical purity of more than 99% was routinely obtained within 25 min of radiosynthesis, including HPLC purification. The total decay-corrected radiochemical yield of [^{11}C]-**1**, based on starting [^{11}C]CH_4, was only 6.5–7.8% ($n = 5$). Addition of 2 equiv of triethylamine did not improve the cyclization reaction yields. No further efforts were made in order to increase the observed low yields. The specific radioactivity measured at the end of the radiosynthesis was 1–2 Ci/μmol (37-74 GBq/μmol).

Formulation of labelled product for *i.v.* injection was effected as follows: (1) HPLC solvent removal by evaporation; (2) reconstitute the residue in 5 mL of physiological saline containing 10% ethanol; (3) sterile filtration through a 0.22 μm filter. The solution for injection was a clear and colourless solution and its pH was between 5 and 7. The preparation was found to be >99% chemically and radiochemically pure, as demonstrated by HPLC analysis. The preparation was free from starting labelling precursor and was shown to be chemically and radiochemically stable for at least 60 min. Administration to animals was done within 15 min following end of synthesis.

2.3. Pharmacology

2.3.1. Radiosensitive β-microprobe acquisition. The brain uptake of [^{11}C]-**1** was investigated in rats using intracerebral radiosensitive β-microprobes[32,33] (Fig. 1A and B). Following *i.v.* injection of [^{11}C]-**1** (0.5–0.8 mCi with specific radioactivity greater than 1 Ci/μmol), the uptake in the cerebellum during the 45 min acquisition was higher than that in the left striatum, 0.50% and 0.35% ID/mL, respectively. In both structures, the radioactive concentration was maximal 2 min post-injection. The washout phase was very slow and similar in both structures. Pre-treatment of rats with EMD-95885 (**1**, 3 mg/kg, *i.p.*, 30 min before injection of the radioligand) resulted in a similar uptake of [^{11}C]-**1** in the cerebellum as in the control experiment at earlier time points, but displayed a faster washout, which was evident as early as 20 min. At 45 min the uptake in the cerebellum was only 0.3% ID/mL compared to 0.5% ID/mL for the control experiment. The uptake of [^{11}C]-**1** in the cerebellum (chosen for its highest accumulation level) was also inhibited by pre-administration of the NR2B prototypic ligand ifenprodil (20 mg/kg, *i.p.*, 30 min before injection of the radioligand) (Fig. 1B). In this case reduction of radioligand uptake was evident as early as 2 min (0.4% ID/mL) followed by washout, which reached levels of 0.3% ID/mL at 45 min.

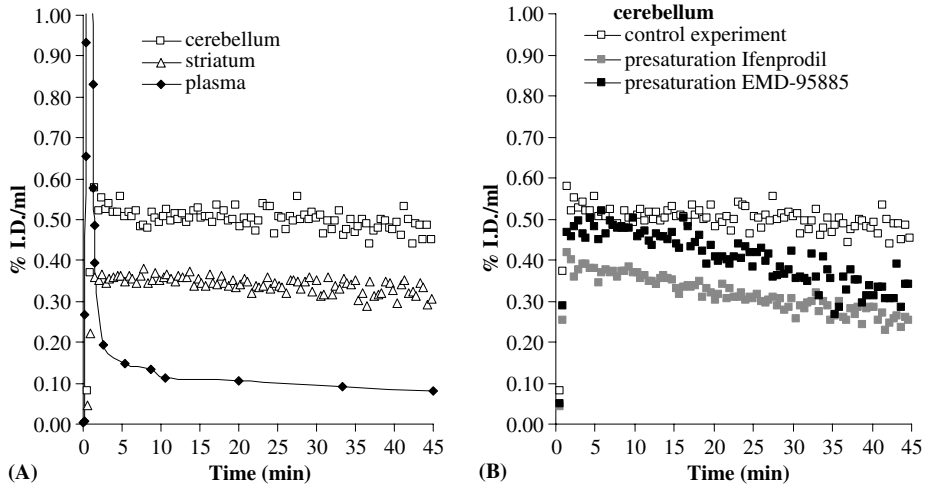

Figure 1. Radiosensitive β-microprobe acquisition: (A) time course of [^{11}C]EMD-95885 ([^{11}C]-**1**) in rat striatum and cerebellum; (B) effect of various drugs on [^{11}C]EMD-95885 ([^{11}C]-**1**) binding in rat cerebellum.

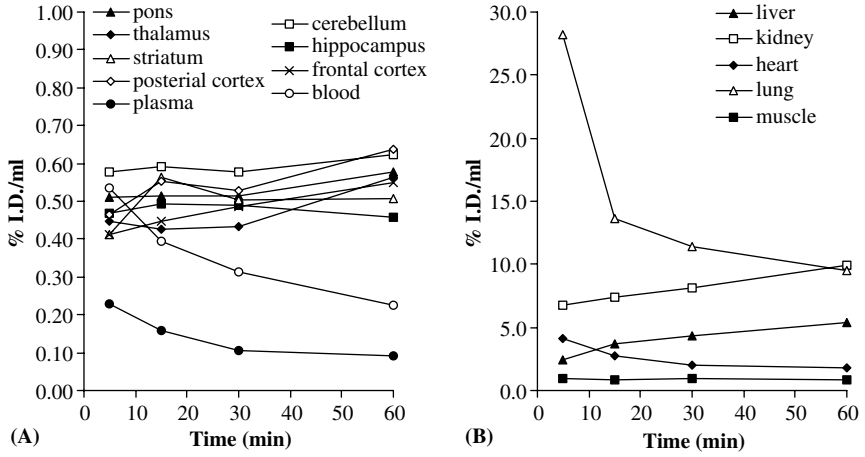

Figure 2. Biodistribution studies in rats: (A) time course of [^{11}C]EMD-95885 ([^{11}C]-**1**) in rat brain; (B) time course of [^{11}C]EMD-95885 ([^{11}C]-**1**) in rat peripheral organs.

2.3.2. Biodistribution studies. Uptake of [^{11}C]-**1** in the rat brain was determined in biodistribution experiments (Fig. 2A). Following *i.v.* injection of [^{11}C]-**1** (22–26 μCi with specific radioactivity greater than 1 Ci/μmol), the distribution was rather homogeneous in all brain structures studied. The uptake in the cerebellum and striatum at 5 min was 0.6% and 0.4% ID/mL, respectively, which was consistent with that observed using the radiosensitive β-microprobes. NR2B subunits are primarily localized in forebrain regions, hippocampus > cortex > striatum > thalamus > cerebellum.[34]

When specific binding was defined as the ratio of the radioactivity concentration in hippocampus and cerebellum, a value of 0.8 was obtained throughout the time course of the experiment. Therefore, the in vivo regional brain distribution of [^{11}C]-**1** did not correlate with the known distribution of NR2B subunits. This uptake does not demonstrate exclusively binding to NR2B subunits but might also reflect in vivo binding to other NMDA receptor subunits including NR2A and NR2C which are expressed in high numbers in the cerebellum.[3,35] In the peripheral organs, the lung showed the highest uptake (28% ID/mL at 5 min) which may reflect a high lipophilicity of **1** ($c\mathrm{Log}P = 4.0$) (Fig. 2B).

In vivo specificity and selectivity of [^{11}C]-**1** binding was examined by studying the effects of ifenprodil (NR2B/σ antagonist), MK801 (NMDA channel blocker), MDL105519 (glycine site antagonist), haloperidol (D2/σ antagonist), and DTG (σ ligand), and the unlabelled drug itself, EMD-95885 (**1**), which were administered at doses of 20, 0.5, 16, 1.5, 2 and 3 mg/kg *i.p.*, respectively, 30 min prior to [^{11}C]-**1** (Fig. 3). Pre-treatment of rats with **1** resulted in a 40–50% global reduction [^{11}C]-**1** uptake demonstrating some specific binding in the brain. Pre-injection of the NR2B ligand ifenprodil reduced the uptake of [^{11}C]-**1** in all brain regions by 46–58%. Although ifenprodil binds to NR2B subunits, the inhibition pattern was inconsistent for this site. Binding to

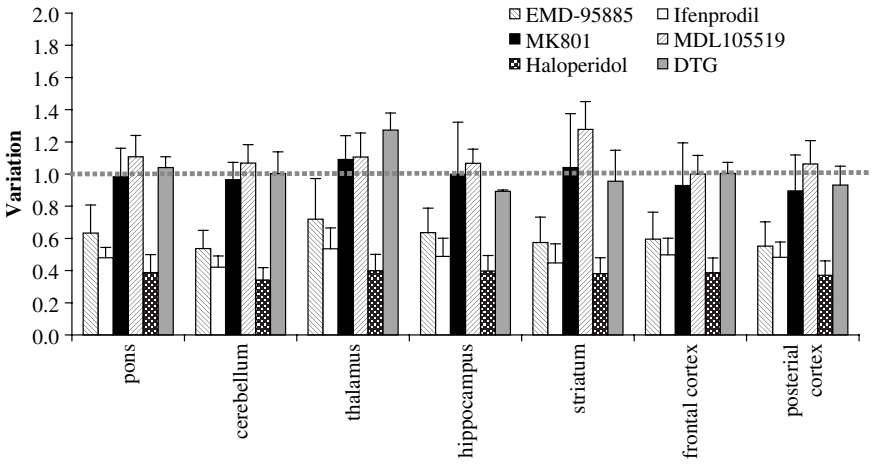

Figure 3. Effect of various drugs on [^{11}C]EMD-95885 ([^{11}C]-**1**) binding in rat brain. Data are means ± SD ($n = 3$).

sigma (σ) receptors was also examined as ifenprodil also shows high affinity for this site ($IC_{50} = 3.9$ nM).[36] The σ ligand DTG had no inhibitory effect on [^{11}C]-**1** binding in any brain region. Pre-treatment with haloperidol resulted in inhibition of [^{11}C]-**1** binding in all brain regions by 60–66%. This does not reflect dopaminergic binding of the radioligand since highest inhibition was observed in the cerebellum (66%), and unlikely to reflect σ receptor binding as the σ ligand DTG had no inhibitory effect on [^{11}C]-**1** uptake in any brain region. However, haloperidol has been reported to block NMDA receptors with efficacy in the low μmol range.[37] This interaction was assumed to be related to interactions with the glycine site[38] with subsequent electrophysiological studies showing that haloperidol specifically inhibited NR2B-containing-NMDA receptors.[39] Nevertheless, the homogeneous pattern of radioligand inhibition displayed by haloperidol is not consistent with selective binding to NR2B subunits. As there are no independent measures on the effect of cerebral blood flow during blocking studies, it is uncertain whether any inhibition observed is a result of specific binding to possibly a combination of subunits, including NR2A and NR2C, or binding at a different site. Pre-treatment of rats with the glycine site antagonist, MDL105519 and the ion channel blocker, MK801, displayed no inhibition of [^{11}C]-**1** uptake indicating that no radioligand binding was evident at these sites.

3. Conclusion

The NR2B subtype-selective antagonist, 6-[3-[4-(4-fluorobenzyl)piperidino]propionyl]-3*H*-benzoxazol-2-one (EMD-95885, **1**), has been synthesized in good yield and labelled with carbon-11 ($T_{1/2}$: 20.4 min) at its benzoxazolinone moiety using [^{11}C]phosgene. The evaluation of its in vivo pharmacological profile (biodistribution studies and brain radioactivity monitoring using intracerebral radiosensitive β-microprobes) clearly indicates that it does not have the required properties for imaging NR2B containing NMDA receptors using positron emission tomography.

4. Experimental

4.1. General

4.1.1. Chemicals, TLCs and HPLCs. Chemicals were purchased from Aldrich and used with no further purification. 4-(4-Fluorobenzyl)piperidine·HCl was a generous gift from Pfizer (Dr. Yuen, Ann Arbor MI). TLCs were run on pre-coated plates of silica gel $60F_{254}$ (Merck) and compounds were visualized at 254 nm using a UV lamp. HPLCs: [HPLC A]: equipment: waters 600 Pump and Waters 600 Controller, a Shimadzu SPD10-AVP UV-multi-wavelength detector; column: Hewlett Packard Zorbax® RX-Sil (250 × 9.4 mm); porosity: 5 μm; eluent CH_2Cl_2/MeOH/aq 28% NH_4OH: 93:7:0.5 (v:v:v); flow rate: 5 mL/min; temperature: rt; absorbance detection at $\lambda = 254$ nm. [HPLC B]: equipment: Waters Alliance 2690 equipped with a UV spectrophotometer (photodiode array detector, Waters 996) and a Berthold LB509 radioactivity detector; column: analytical Symmetry-M® C-18, Waters (4.6 × 50 mm); porosity: 3.5 μm; conditions: isocratic elution with solvent A/solvent B: 39:61 (v:v) [solvent A: H_2O containing low-UV PIC® B7 reagent (waters, % by weight: methanol (18–22%), heptane sulfonic acid–sodium salts (4–6%), phosphate buffer solution (3–7%), water (65–75%), pH 3), 20 mL for 1000 mL; solvent B: H_2O/CH_3CN: 50:50 (v:v) containing low-UV PIC® B7 reagent, 20 mL for 1000 mL]; flow rate: 2.0 mL/min; temperature: 30 °C; absorbance detection at $\lambda = 254$ nm.

4.1.2. Spectroscopies. NMR spectra were recorded on a Varian Gemini (300 MHz) instrument using the hydrogenated residue of the deuteriated solvents ($CDCl_3$, $\delta = 7.26$ ppm; CD_3OD, $\delta = 3.34$ and 4.11 ppm) and/or TMS as internal standard for ^{1}H NMR. The chemical shifts are reported in ppm downfield from TMS (br m, d, dd, dt, m, t; broad multiplet, doublet, doublet of doublet, doublet of triplet, multiplet and triplet, respectively). The mass spectra MS were recorded on a Finnigan/MAT TSQ46 using electron impact.

4.1.3. Radioisotope production. No-carrier-added $[^{11}C]CH_4$ was produced on a CGR-MeV 520 cyclotron by irradiation of a target consisting of an ultrapure Air Liquide 95/5 mixture of N_2/H_2 (target holder: 668 mL operated at 8 bars) using a 20 MeV proton beam by the $^{14}N[p, \alpha]^{11}C$ nuclear reaction. Typical production: 1.20 Ci (44.40 GBq) of $[^{11}C]CH_4$ at the end of bombardment (EOB) for a 30 μA, 30 min (54,000 μC) irradiation.

4.1.4. Miscellaneous. Radiosyntheses using carbon-11, including the HPLC purifications, were performed in a 5 cm-lead shielded cell. Specific radioactivity was determined as follows: the area of the absorbance peak corresponding to the radiolabelled product was measured on the HPLC chromatogram and compared to a standard curve relating mass to absorbance.

4.2. Chemistry

4.2.1. 6-(3-Chloropropionyl)-3*H*-benzoxazol-2-one (4). Dimethylformamide (6.0 mL, 80 mmol) was slowly added to aluminium chloride (37.3 g, 280 mmol) while stirring and maintaining a temperature of 45 °C. To the mixture was then added 2-benzoxazolinone (**3**, 5.4 g, 40 mmol) and 3-chloropropionyl chloride (6.2 g, 60 mmol) followed by warming at 75 °C for 2 h. The reaction mixture was then poured on ice and the crude product (4.6 g) was collected by filtration, air-dried and recrystallized from dioxane. This yielded the title compound (**4**) as a white solid (2.6 g, 29%). ^1H NMR ($CDCl_3$) δ: 3.45 (m, 2H); 3.95 (m, 2H); 7.2 (m, 2H); 7.9 (m, 2H); 8.6 (br m, 1H).

4.2.2. 6-[3-[4-(4-Fluorobenzyl)piperidino]propionyl]-3*H*-benzoxazol-2-one (1). 4-(4-Fluorobenzyl)piperidine·HCl (1.0 g, 4.4 mmol) and NEt_3 (1.3 mL, 9.3 mmol) were added to a suspension of 6-(3-chloropropionyl)-3*H*-benzoxazol-2-one (**4**, 1.0 g, 4.4 mmol) in EtOH (10 mL). The mixture was stirred at room temperature for 2 h and then basified using excess NEt_3. The reaction mixture was concentrated by rotary evaporation and the residue suspended in isopropanol. The resulting solid was filtered and washed with water and isopropanol and air-dried to yield the title compound (1) as a white powder (1.2 g, 71%). ^1H NMR ($CDCl_3$) δ: 1.3 (m, 2H); 1.5 (m, 1H); 1.65 (d, $J = 12.6$ Hz, 2H); 2.0 (m, 2H); 2.5 (d, $J = 6.9$ Hz, 2H); 2.8 (t, $J = 7.4$ Hz, 2H); 2.95 (d, $J = 11.4$ Hz, 2H); 3.2 (t, $J = 7.4$ Hz, 2H); 6.95 (m, 2H); 7.15 (m, 3H); 7.8 (m, 2H).

The free base was converted into its HCl salt by suspending 6-[3-[4-(4-fluorobenzyl)piperidino]propionyl]-3*H*-benzoxazol-2-one (**1**, 0.3 g, 0.8 mmol) in a mixture of isopropanol (3 mL) and diethyl ether saturated with HCl (2 mL). The suspension was filtered and the solid washed with small amounts of anhydrous diethyl ether to give the HCl salt of (**1**) as a white powder (0.2 g, 67%). ^1H NMR (CD_3OD) δ: 1.5 (m, 2H); 1.9 (m, 3H); 2.6 (d, $J = 6.6$ Hz, 2H); 3.0 (t, $J = 11.7$ Hz, 2H); 3.5–3.7 (m, 6H); 7.0 (t, $J = 8.6$ Hz, 2H); 7.2 (m, 3H); 7.9 (d, $J = 1.8$ Hz, 1H); 7.9 (dd, $J = 1.8$, 8.6 Hz, 1H). MS: $C_{22}H_{23}F_1N_2O_3$: 383 [M+1].

4.2.3. (4-[3-[4-(4-Fluorobenzyl)piperidino]propionyl]-2-hydroxy-phenyl)-carbamic acid *tert*-butyl ester (5). 6-[3-[4-(4-Fluorobenzyl)piperidino]propionyl]-3*H*-benzoxazol-2-one (**1**, 0.3 g, 0.7 mmol), NEt_3 (0.1 mL, 0.9 mmol) and DMAP (19 mg, 0.2 mmol) were dissolved in THF (7 mL). To the mixture was then added di-*tert*-butyl dicarbonate (0.2 g, 1.0 mmol) in three portions over 10 min and the mixture was stirred at room temperature for 2 h. The reaction mixture was concentrated in vacuo to give a light-yellow oil, to which was added MeOH (6 mL) followed by stirring for an additional 40 min at room temperature. A light-yellow precipitate was formed to which was added K_2CO_3 (107 mg, 0.8 mmol) and stirring was continued for 1.5 h. The mixture was concentrated by evaporation to reduce the volume of MeOH and water was added resulting in an suspension, which was partitioned with EtOAc and water. The organic phase was filtered through silica gel (1.9 g) to give a light-yellow clear solution, which was concentrated in vacuo to give the title compound (**5**) as a light-yellow oil, which solidified on cooling (0.3 g, 89%). ^1H NMR ($CDCl_3$): 1.2–1.4 (m, 2H); 1.5 (m, 10H); 1.6–1.8 (d, $J = 12.6$ Hz, 2H); 2.0–2.2 (t, $J = 11.4$ Hz, 2H); 2.5 (d, $J = 6.9$ Hz, 2H); 2.9 (t, $J = 7.4$ Hz, 2H); 3.1 (d, $J = 11.4$ Hz, 2H); 3.2 (t, $J = 7.4$ Hz, 2H); 6.95 (m, 2H); 7.1 (m, 2H); 7.4 (m, 2H); 7.9 (d, $J = 10.5$ Hz, 1H).

4.2.4. 1-(4-Amino-3-hydroxy-phenyl)-3-[4-(4-fluorobenzyl)piperidin-1-yl]propan-1-one (2). A suspension of (4-[3-[4-(4-fluorobenzyl)piperidino]propionyl]-2-hydroxy-phenyl)-carbamic acid *tert*-butyl ester (**5**, 0.3 g, 0.7 mmol) in CH_2Cl_2 (6.9 mL) was cooled to 0 °C. Trifluoroacetic acid (0.7 mL) was added and the resulting light-brown solution was stirred for 0.5 h at 0 °C and then for 4 h at room temperature. The reaction mixture was evaporated to dryness and basified with a concentrated Na_2CO_3 solution, then extracted with CH_2Cl_2. The organic layer was dried with Na_2SO_4 and evaporated in vacuo and the residue was purified by column chromatography to yield the title compound as a brown solid (0.2 g, 80%). ^1H NMR ($CDCl_3$) δ: 1.4 (dt, $J = 3.6$, 12.6 Hz, 2H); 1.5 (m, 1H); 1.65 (d, $J = 12.6$ Hz, 2H); 2.0–2.2 (t, $J = 11.4$ Hz, 2H); 2.5 (d, $J = 6.9$ Hz, 2H); 2.85 (t, $J = 7.4$ Hz, 2H); 3.05 (d, $J = 11.4$ Hz, 2H); 3.15 (t, $J = 7.4$ Hz, 2H); 6.65 (d, $J = 8.7$ Hz, 1H); 6.95 (t, $J = 8.7$ Hz, 2H); 7.05 (dd, $J = 5.4$, 8.7 Hz, 2H); 7.4 (m, 2H). MS: $C_{21}H_{25}F_1N_2O_2$: 357 [M+1].

4.3. Radiochemistry

4.3.1. Preparation of $[^{11}C]CCl_4$. At the end of the bombardment, the target contents were transferred by expansion to the 5 cm-lead shielded hot cell dedicated to the radiosynthesis of the tracer and passed firstly through an empty tube (stainless steel coil, 500 mm length, 4 mm internal diameter, cooled at −186 °C using

liquid argon) in order to remove traces of ^{13}N-ammonia (produced during the irradiation) and secondly through a guard of P_2O_5 (glass tube, 70 mm length, 3 mm internal diameter) in order to remove moisture. [^{11}C]CH_4 was then separated from the target gas by trapping in a copper-U-tube (150 mm length, 4 mm internal diameter) filled with Porapak-Q (80–100 mesh, Waters) and cooled at −186 °C (liquid argon). [^{11}C]CH_4 was released from the trap by warming the copper-U-tube to room temperature (hot air) and swept away by a flow of helium gas (40 mL/min). [^{11}C]CH_4 was then passed through a guard of P_2O_5 (glass tube, 70 mm length, 10 mm internal diameter) and concentrated in a second smaller copper-U-tube (150 mm length, 2 mm internal diameter) filled with Porapak-Q (80–100 mesh, Waters) and cooled at −186 °C (liquid argon). On average, about 1.20 Ci or 44.40 GBq (at EOB) of [^{11}C]CH_4 is routinely produced for a 30 μA, 30 min (54,000 μC) irradiation and then transferred and concentrated in 4–5 min using the process described above. [^{11}C]CH_4 was released from the trap by warming the latter to room temperature and swept (15 mL/min) in a volume of 1–2 mL of helium into a gas mixing chamber containing 3 mL of chlorine (99.99%, Air Liquide). Using the same helium as vector gas (15 mL/min), the [^{11}C]CH_4-chlorine mixture was passed through an empty horizontal glass tube (215 mm length, 7 mm internal diameter) at a temperature of 510 °C converting [^{11}C]CH_4 into [^{11}C]CCl_4.

4.3.2. Preparation of [^{11}C]$COCl_2$. The synthesized [^{11}C]CCl_4 was then on-line passed through a glass-U-tube (200 mm length, 4 mm internal diameter) containing 1.5 g of iron filings (Telar 57, Weber) at a temperature of 290–310 °C (using the [^{11}C]CCl_4 vector gas) converting it into [^{11}C]$COCl_2$, which was then passed through an antimony-guard (glass tube, 70 mm length, 3 mm internal diameter, containing a 2/1 ratio [v/v] of antimony powder (400 mg) and glass beads (1 mm diameter) in order to remove the excess of chlorine.

4.3.3. Preparation of 6-[3-[4-(4-fluorobenzyl)piperidino]-propionyl]-3*H*-benzoxazol-2-[^{11}C]one ([^{11}C]-1). The on-line synthesized [^{11}C]$COCl_2$ was trapped (bubbling through) at room temperature in a reaction vessel containing 0.5–1.0 mg of the labelling precursor 1-(4-amino-3-hydroxy-phenyl)-3-[4-(4-fluoro-benzyl)-piperidin-1-yl]-propan-1-one (**2**, 1.4–2.8 μmol) dissolved in 500 μL of CH_2Cl_2. Trapping of [^{11}C]$COCl_2$ was monitored using an ionization-chamber probe. When the reading had reached its maximum (2–3 min usually), the reaction mixture was diluted with 1.0 mL of HPLC solvent and injected onto the column. (HPLC A; t_R: [^{11}C]-**1**: 7.0–7.5 min).

4.3.4. Formulation of 6-[3-[4-(4-fluorobenzyl)piperidino]-propionyl]-3*H*-benzoxazol-2-[^{11}C]one ([^{11}C]-1). Formulation of labelled product for *i.v.* injection was effected as follows: The HPLC-collected fraction containing [^{11}C]-**1** was concentrated to dryness (using a rotavapor, water bath temperature: 40–60 °C or using a helium gas stream, oil bath temperature: 70–80 °C). The residue was taken up in 2–5 mL of physiological saline containing 10% of ethanol and filtered through a sterile 0.22 μm filter into a sterile, pyrogen free evacuated vial.

4.3.5. Quality control of 6-[3-[4-(4-fluorobenzyl)piperidino]propionyl]-3*H*-benzoxazol-2-[^{11}C]one ([^{11}C]-1). The radioligand preparation is a clear and colourless solution and its pH is between 5 and 7. As demonstrated by HPLC analysis (HPLC B), the radiolabelled product was found to be >98% radiochemically pure (HPLC B; retention time: 3.12 min). The preparation was shown to be free of nonradioactive precursor and radiochemically stable for at least 60 min. Specific radioactivity was calculated from three consecutive HPLC analyses (average) and determined as follows: The area of the UV absorbance peak corresponding to the radiolabelled product was measured (integrated) on the HPLC chromatogram and compared to a standard curve relating mass to UV absorbance. The first injection in animal experiments was done within 15 min after the end of synthesis.

4.4. Kinetics, regional distribution and radiopharmacological characterization in rodents

4.4.1. Animals. Sprague–Dawley male rats weighing 250–350 g were used in all experiments. Animals use procedures were in accordance with the recommendations of the EEC (86/609/CEE) and the French National Committee (decret 87/848) for the care and use of laboratory animals.

4.4.2. Intracerebral radiosensitive β-microprobes acquisition. Anaesthesia of animals was induced with 5% isoflurane in a gas mixture of O_2/N_2O (30/70%) and maintained with 1.5–2.5% isoflurane during the entire surgical procedure. Body temperature was monitored rectally and maintained by means of a thermoregulated blanket. Catheters were placed in both femoral vein and artery. Animals were then mounted in a stereotaxic frame. Craniotomies were performed in order to implant the radiosensitive β-microprobes (Biospace Mesures, Paris). Two probes were implanted, the first one in the left striatum and the second one in the cerebellum using the coordinates of implantation according to the atlas of Paxinos and Watson.[40] Data were acquired from 30 min after probes implantation. Local radioactivity count rates were acquired for 30 min prior to the radioligand injection to evaluate environmental background (approximately 5 cps) with a temporal resolution of 1 s. In control experiments, the radioligand was injected in the femoral vein ([^{11}C]-**1**, 0.5–0.8 mCi) in a volume of 1 mL over 1 min. Data were acquired for another 45 min with a temporal resolution of 1 s. Finally, mean background noise was subtracted from the raw data and radioactive decay correction for carbon-11 was applied to obtain quantitative time activity curves. Samples of plasma were also obtained for each animal. Results were expressed as %injected dose per mL (% ID/mL). In vivo

receptor blocking studies were performed by pre-administration, 30 min before injection of the radioligand, of EMD-95885 (**1**, 3 mg/kg, *i.p.*) or ifenprodil (20 mg/kg, *i.p.*).

4.4.3. Biodistribution studies. Each animal received 15–30 μCi of the radioligand ([^{11}C]-**1**), dissolved in 0.1 mL saline, by injection in a tail vein. At designated times (5, 15, 30, 60 min) after injection of the radioligand, animals ($n = 3$ per time point) were killed by decapitation, the brains as well as peripheral organs were quickly removed, dissected, weighed and assayed for radioactivity in a γ-counter (Cobra Quantum, Packard). Samples of liver, kidney, heart, lung, muscle, blood, plasma and for the brain, pons, cerebellum, thalamus, hippocampus, striatum, frontal cortex, posterial cortex were obtained for each animal. Results were expressed as %injected dose per mL (% ID/mL) after correction for the physical decay of the radioisotope. In vivo receptor blocking studies were also performed on three animals by pre-administration, 30 min before injection of the radioligand, of EMD-95885 (**1**, 3 mg/kg, *i.p.*), ifenprodil (20 mg/kg, *i.p.*), MK-801 (0.5 mg/kg, *i.p.*), MDL-105519 (16 mg/kg, *i.p.*), haloperidol (1.5 mg/kg, *i.p.*) or 1,3-di-*ortho*-tolylguanidine (DTG, 2 mg/kg, *i.v.*). Animals were then *i.v.*-injected with the radioligand ([^{11}C]-**1**, 15–20 μCi in 0.1 mL saline) and sacrificed 30 min later. The brain was dissected as mentioned above. Results were expressed as % of variation compared to the controls after correction for the physical decay of the radioisotope and correction of plasma variation.

Acknowledgements

The authors wish to thank the cyclotron operators Mr. Daniel Gouel, Mr. Christophe Peronne and Mr. Christophe Lechêne for performing the irradiations. The authors also wish to thank Dr. Dirk Roeda for proofreading the manuscript.

References and notes

1. Dingledine, R.; Borges, K.; Bowie, D.; Traynelis, S. *Pharmacol. Rev.* **1999**, *51*, 7.
2. Johnson, J.; Ascher, P. *Nature* **1987**, *325*, 529.
3. Seeberg, P. *Trends Neurosci.* **1993**, *16*, 359.
4. Laube, B.; Hirai, H.; Sturgess, M.; Betz, H.; Kuhse, J. *Neuron* **1997**, *18*, 493.
5. Kuryatov, A.; Laube, B.; Betz, H.; Kuhse, J. *Neuron* **1994**, *12*, 1291.
6. Danysz, W.; Parsons, C. *Pharmacol. Rev.* **1998**, *50*, 597.
7. Le, D.; Lipton, S. *Drugs Aging* **2001**, *18*, 717.
8. Nikam, S.; Meltzer, L. *Curr. Pharm. Des.* **2002**, *8*, 845.
9. Chenard, B. L.; Menniti, F. S. *Curr. Pharm. Des.* **1999**, *5*, 381.
10. Frost, J., Jr.; Wagner, H. *Quantitative Imaging- Neuroreceptors, Neurotransmitters and Enzymes*; Raven: New York, 1990.
11. Haradahira, T.; Okauchi, T.; Maeda, J.; Zhang, M.-R.; Nishikawa, T.; Konno, R.; Suzuki, K.; Suhara, T. *Synapse* **2003**, *50*, 130.
12. Haradahira, T.; Okauchi, T.; Maeda, J.; Zhang, M.-R.; Kida, T.; Kawabe, K.; Mishina, M.; Watanabe, Y.; Suzuki, K.; Suhara, T. *Synapse* **2002**, *43*, 131.
13. Waterhouse, R.; Sultana, A.; Laruelle, M. *Nucl. Med. Biol.* **2002**, *29*, 791.
14. Haradahira, T.; Zhang, M.-R.; Maeda, J.; Okauchi, T.; Kida, T.; Kawabe, K.; Sasaki, S.; Suhara, T.; Suzuki, K. *Chem. Pharm. Bull. Tokyo* **2001**, *49*, 147.
15. Kokic, M.; Honer, M.; Kessler, L.; Grauert, M.; Schubiger, P.; Ametamey, S. *J. Recept. Signal Transduct* **2002**, *22*, 123.
16. Ishibashi, N.; Kuwamura, T.; Sano, H.; Yamamoto, F.; Haradahira, T.; Suzuki, K.; Suhara, T.; Sasaki, S.; Maeda, J. *J. Lab.Compd. Radiopharm.* **2000**, *43*, 375.
17. Haradahira, T.; Sasaki, S.; Maeda, J.; Kobayashi, K.; Inoue, O.; Tomita, U.; Nishikawa, T.; Suzuki, K. *J. Lab.Compd. Radiopharm.* **1998**, *41*, 843.
18. Sihver, S.; Sihver, W.; Andersson, Y.; Murata, T.; Bergstrom, M.; Onoe, H.; Matsumura, K.; Tsukada, H.; Oreland, L.; Långström, B.; Watanabe, Y. *J. Neural. Trans.* **1998**, *105*, 117.
19. Andersson, Y.; Tyrefors, N.; Sihver, S.; Onoe, H.; Watanave, Y.; Tsukada, H.; Långström, B. *J. Lab.Compd. Radiopharm.* **1998**, *41*, 567.
20. Haradahira, T.; Maeda, J.; Okauchi, T.; Zhang, M.-R.; Hojo, J.; Kida, T.; Arai, T.; Yamamoto, F.; Sasaki, S.; Maeda, M.; Suzuki, K.; Suhara, T. *Nucl. Med. Biol.* **2002**, *29*, 517.
21. Roger, G.; Lagnel, B.; Besret, L.; Bramoulle, Y.; Coulon, C.; Ottaviani, M.; Kassiou, M.; Bottlaender, M.; Valette, H.; Dolle, F. *Bioorg. Med. Chem.* **2003**, *11*, 5401.
22. Leibrock, J.; Prucher, H.; Rautenberg, W. *Pharmazie* **1997**, *52*, 479.
23. Prucher, H.; Gottschlich, R.; Leibrock, J. WO Patent 98/18793, 1998.
24. Baine, N.; Clark, W., Jr.; Eldridge, A. WO Patent 00/12468, 2000.
25. Aichaoui, H.; Lesieur, D.; Henichart, J.-P. *J. Heterocycl. Chem.* **1992**, *29*, 171.
26. Moussavi, Z.; Lesieur, D.; Lespagnol, C.; Sauzieres, J.; Olivier, P. *Eur. J. Med. Chem.* **1989**, *24*, 55.
27. Bonte, J.-P.; Lesieur, D.; Lespagnol, C.; Cazin, J.-C.; Cazin, M. *Eur. J. Med. Chem.* **1974**, *9*, 497.
28. Dollé, F.; Valette, H.; Bramoulle, Y.; Guenther, I.; Fuseau, C.; Coulon, C.; Lartizien, C.; Jegham, S.; George, P.; Curet, O.; Pinquier, J.-L.; Bottlaender, M. *Bioorg. Med. Chem. Lett.* **2003**, *13*, 1771.
29. Dollé, F.; Bramoulle, Y.; Hinnen, F.; Demphel, S.; George, P.; Bottlaender, M. *J. Lab. Compd. Radiopharm.* **2003**, *46*, 783.
30. Link, J.; Krohn, K. *J. Lab. Compd. Radiopharm.* **1997**, *40*, 306.
31. Landais, P.; Crouzel, C. *Appl. Radiat. Isot.* **1987**, *38*, 297.
32. Pain, F.; Laniece, P.; Mastrippolito, R.; Pinot, L.; Charon, Y.; Glatiny, A.; Guillemin, M.; Hantraye, P.; Leviel, V.; Menard, L.; Valentin, L. *IEEE Trans. Nucl. Med.* **2002**, *49*, 822.
33. Zimmer, L.; Hassoun, W.; Pain, F.; Bonnefoi, F.; Laniece, P.; Mastrippolito, R.; Pinot, L.; Pujol, J.; Leviel, V. *J. Nucl. Med.* **2002**, *43*, 227.
34. Mutel, V.; Buchy, D.; Klingelschmidt, A.; Messer, J.; Bleuel, Z.; Kemp, J. A.; Richards, J. G. *J. Neurochem.* **1998**, *70*, 2147.
35. Monyer, H.; Burnashev, N.; Laurie, D.; Sakmann, B.; Seeberg, P. *Neuron* **1994**, *12*, 529.
36. Chenard, B.; Shalaby, I.; Koe, B.; Ronau, R.; Butler, T.; Prochniak, M.; Schmidt, A.; Fox, A. *J. Med. Chem.* **1991**, *34*, 3085.

37. Monnet, F.; Debonnel, G.; Juien, J.-L.; De Montigny, C. *Eur. J. Pharmacol.* **1990**, *179*, 441.
38. Fletcher, E.; MacDonald, J. *Eur. J. Pharmacol.* **1993**, *235*, 291.
39. Coughenour, L. L.; Cordon, J. J. *Pharmacol. Exp. Ther.* **1997**, *280*, 584.
40. Paxinos, G.; Watson, C. *The Rat Brain in Stereotaxic Coordinates*; Academic: New York, 1986.